

DiPolMol-Py: A Python package for calculations for $^2\Sigma$ ground-state molecules

Bethan Humphreys^a, Alex J. Matthies^a, Hannah J. Williams^{a,*}

^a*Department of Physics, Durham University, South Road, Durham DH1 3LE, United Kingdom*

Abstract

We present the python package DiPolMol-Py, which can be used to calculate the rotational and hyperfine structure of $^2\Sigma$ molecules. The calculations can be performed in the presence of dc magnetic fields, dc electric fields and far off-resonant optical fields. We additionally include functions to calculate the polarisability of the molecule and the transition dipole moment between different energy eigenstates. The package is applicable to many of the molecules which can be laser cooled, specifically the alkaline earth fluorides. We provide a constants file which includes many of the required literature values for CaF, SrF and BaF. Additional species can easily be added by updating this file.

PROGRAM SUMMARY

Program Title: DiPolMol-Py

CPC Library link to program files: (to be added by Technical Editor)

Developer's repository link: <https://github.com/durham-qlm/DiPolMol>

Licensing provisions: BSD 3-clause

Programming language: Python ≥ 3.11

Nature of problem: Calculating the rotational and hyperfine structure for $^2\Sigma$ ground state molecules both field free and in the presence of dc magnetic, electric and off-resonant light fields.

Solution method: A Python package which calculates the eigenenergies and eigenvalues via diagonalisation of the Hamiltonian.

Additional comments including restrictions and unusual features (approx. 50-250 words):

*Corresponding author.

E-mail address: hannah.williams4@durham.ac.uk

This package is based on previous work for $^1\Sigma$ molecules [1]. External magnetic and electric fields must be coaxial.

References

- [1] J. A. Blackmore, P. D. Gregory, J. M. Hutson, S. L. Cornish, *Computer Physics Communications* 282 (2023) 108512. doi:10.1016/j.cpc.2022.108512.

Ultracold molecules offer many exciting opportunities from fundamental science to quantum technologies, made possible by their complex internal structure. Transitions between internal energy levels can be used as sensitive probes to search for variations in fundamental constants or beyond standard model physics, e.g. electrons electric dipole moment [1, 2, 3, 4], nuclear Schiff moment [5], and electron-to-proton mass ratio [6]. The long-range, tuneable dipole-dipole interactions present between rotational levels allow for the entanglement of molecules [7, 8, 9, 10, 11], which combined with long-coherence times [12, 13, 14, 15] make molecules a promising platform for quantum computing and simulation [16, 17, 18, 19, 20]. The rotational level structure extends the capabilities of such platforms to include synthetic dimensions [21, 22] or qudits [23]. With the ability to control internal and external degrees of freedom, cold molecules are also ideal for the study of cold, controlled chemistry [24, 25, 26] and collisions [27, 28, 29].

Direct laser cooling of molecules is one way of producing ultracold samples of molecules. It was first proposed in 2004 [30], and since then the field has advanced rapidly. The first molecular magneto-optical trap (MOT) was demonstrated in 2014 using strontium monofluoride (SrF) [31], with several further species being trapped since (CaF [32, 33], YO [34], CaOH [35], SrOH [36], ^{138}BaF [37]). Even more are being investigated currently (YbF [38], ^{137}BaF [39], CaH [40], CaD [41], MgF [42], AlF [43], TlF [44], CH [45]).

Implementing any of the potential applications of molecules requires an accurate understanding of the internal energy level structure, both with and without the presence of external fields. A Python package *diatom.py* [46] was recently written to calculate the rotational and hyperfine structure of $^1\Sigma$ molecules, applicable typically to associated, alkali molecules. In this paper we present a complementary Python package *DiPolMol.py* which works for $^2\Sigma$ molecules, and is thus applicable to many laser-coolable diatomic molecules.

We provide most¹ of the required constants to calculate the structure of CaF, SrF and BaF. As more species are investigated, and the required constants become known, these can be added to the programme. This could include associated molecules such as RbSr [47], RbYb [48], CsYb [49] or LiYb [50] which similarly have a $^2\Sigma$ ground state.

The remainder of this paper is structured as follows. Section (Theory) outlines the Hamiltonian used in the calculations; considering rotational and hyperfine structure as well as the effect of external magnetic and electric fields. Section (Package) outlines how the code is structured and how the user can perform calculations. Finally, section (Examples) demonstrates an application of the DiPolMol-Py package to CaF, SrF and BaF to calculate polarisability, Zeeman shifts, ac and dc electric field shifts and transition dipole moments between different rotational states.

1. Theory

In this package we consider a molecule in the ground electronic and vibrational state. The total Hamiltonian describing such a molecule is

$$H_{\text{tot}} = H_{\text{rot}} + H_{\text{hf}} + H_{\text{ext}}, \quad (1)$$

where H_{rot} and H_{hf} give the field-free rotational and hyperfine structure, respectively, and H_{ext} describes the interaction with external electric, magnetic and off-resonant light fields. We give the Hamiltonian in Eqn. 1 using dimensionless operators for electron spin, $\hat{\mathbf{S}}$, nuclear spin, $\hat{\mathbf{I}}$ and rotational angular momentum $\hat{\mathbf{N}}$. In the package we use the matrix representation of the Hamiltonian to calculate the associated energy shifts. The matrix representation for each Hamiltonian is presented in the Appendix.

1.1. Basis

The electronic ground state for most molecules which are being pursued as candidates for laser cooling is $^2\Sigma$. The term symbol is given by $^{2S+1}\Lambda$, where S is the total electronic spin angular momentum and Λ is the projection of the total electronic orbital angular momentum L onto the internuclear axis.

¹Constants for SrF and BaF light shift and polarisability could not be found in literature.

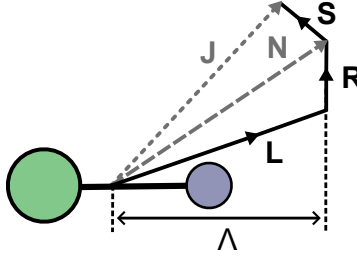


Figure 1: Illustration of Hund's case (b) angular momentum couplings. The orbital angular momentum \mathbf{L} and the rotational angular momentum \mathbf{R} couple to form \mathbf{N} , which in turn couples to the spin angular momentum \mathbf{S} , forming \mathbf{J} . The projection of the orbital angular momentum onto the internuclear axis is given by Λ , as shown.

Values of $\Lambda = 0, 1, 2, \dots$ are represented by $\Lambda = \Sigma, \Pi, \Delta, \dots$. Thus, molecules in ${}^2\Sigma$ states have $S = \frac{1}{2}$ and $\Lambda = L = 0$.

Hund's case (b) best describes this system whereby the rotational angular momentum R is first coupled to the electronic angular momentum L to make $N = L + R$. N is then coupled with electronic spin S to give the total angular momentum $J = N + S$. The coupling scheme is illustrated in figure 1. Note that as we consider molecules in the ${}^2\Sigma$ state, N only has a contribution from the rotational angular momentum, i.e., $N = R$. The total angular momentum J couples with the nuclear spin I , to give the hyperfine structure with $F = J + I$. The projection of the angular momentum F onto the internuclear axis is given by m_F . The natural state basis is thus the coupled regime $|N, J, F, m_F\rangle$.

1.2. Rotational Hamiltonian

The molecular rotation can be approximated by the rigid-rotor model, resulting in an array of rotational states spaced in energy according to $E_N \approx B_v N(N+1)$, where B_v is the rotational constant in vibrational level v . However, this approximation does not hold for large N . At faster rates of rotation there is an increase in the centrifugal force which causes the bond length to grow. This effect is captured by the centrifugal distortion coefficient D_v , which is typically six orders of magnitude smaller than B_v . The rotational Hamiltonian is [51]

$$H_{\text{rot}} = B_v(\hat{\mathbf{N}} \cdot \hat{\mathbf{N}}) - D_v(\hat{\mathbf{N}} \cdot \hat{\mathbf{N}})^2. \quad (2)$$

1.3. Hyperfine Hamiltonian

In this package, we consider only those molecules where one of the constituent atoms has no nuclear spin, i.e., for a molecule AB $I_A = 0$ and $I_{AB} = I_B$. This is the case for molecules containing ^{40}Ca , ^{88}Sr or ^{138}Ba and covers the majority of molecules currently being investigated for laser cooling. The hyperfine Hamiltonian takes the form

$$H_{\text{hf}} = H_{\text{e spin-rot}} + H_{\text{spin-spin}} + H_{\text{n spin-rot}}. \quad (3)$$

The first term describes the electronic spin-rotation interaction and is given by

$$H_{\text{e spin-rot}} = \gamma \hat{\mathbf{S}} \cdot \hat{\mathbf{N}}, \quad (4)$$

where γ is the electron spin-rotational coupling constant.

The second term describes the interaction between the electronic and nuclear magnetic moments and can be decomposed into a scalar and a tensor part. These are written as

$$H_{\text{spin-spin}}^{(0)} = (b + c/3) \hat{\mathbf{I}} \cdot \hat{\mathbf{S}}, \quad (5)$$

$$H_{\text{spin-spin}}^{(2)} = (c/3) \sqrt{6} T^2(C) \cdot T^2(\hat{\mathbf{I}}, \hat{\mathbf{S}}), \quad (6)$$

with spectroscopic constants b and c [52]. $T^2(C)$ and $T^2(\hat{\mathbf{I}}, \hat{\mathbf{S}})$ are rank-2 spherical tensors where (C) represents the renormalised spherical harmonics $C_q^2(\theta, \phi)$.

The final term is the nuclear spin-rotation interaction, written as

$$H_{\text{n spin-rot}} = c_{\text{F}} \hat{\mathbf{I}} \cdot \hat{\mathbf{N}}. \quad (7)$$

The nuclear interaction is typically three orders of magnitude smaller than the others, with constant c_{F} ².

1.4. External Hamiltonian

We next consider the interaction between the molecule and an external electromagnetic field. We introduce $\boldsymbol{\lambda}$ as a unit vector along the internuclear axis in the direction from negative to positive charge (e.g., from the F to the Ca in CaF). The total external Hamiltonian can be expressed as the

²Sometimes referred to as C .

sum of three Hamiltonians which describe the effect of magnetic, electric and off-resonant optical fields. The total external Hamiltonian is therefore

$$H_{\text{ext}} = H_{\text{B}} + H_{\text{dc}} + H_{\text{ac}}. \quad (8)$$

An external magnetic field \mathbf{B} leads to a splitting in energy levels described by the Zeeman Hamiltonian, which can be expressed as [51]

$$H_{\text{B}} = g_s \mu_{\text{B}} \hat{\mathbf{S}} \cdot \mathbf{B} + g_l \mu_{\text{B}} [\hat{\mathbf{S}} \cdot \mathbf{B} - (\hat{\mathbf{S}} \cdot \boldsymbol{\lambda})(\mathbf{B} \cdot \boldsymbol{\lambda})] \\ - g_r \mu_{\text{B}} \hat{\mathbf{N}} \cdot \mathbf{B} - g_{\text{N}} \mu_{\text{N}} \hat{\mathbf{I}} \cdot \mathbf{B}, \quad (9)$$

where the first term is generally three orders of magnitude larger than the others. The four terms describe the contributions of the electron's magnetic dipole moment, the anisotropic correction to this, the rotation of the electron, and the nuclear magnetic moment respectively. These terms are characterised by their associated g -factors g_s , g_l , g_r and g_{N} .

The permanent electric dipole moment μ_{e} of a molecule couples to an external dc electric field \mathbf{E}_{dc} . The Hamiltonian describing this interaction is

$$H_{\text{dc}} = -\mu_{\text{e}} \mathbf{E}_{\text{dc}} \cdot \boldsymbol{\lambda}. \quad (10)$$

Finally, we include the interactions between the molecule and a non-resonant light field. Here the dipole moment operator of the molecule $\hat{\mathbf{d}}$ interacts with the ac electric field of the light \mathbf{E}_{ac} . The associated Hamiltonian is written as

$$H_{\text{ac}} = -\hat{\mathbf{d}} \cdot \mathbf{E}_{\text{ac}}. \quad (11)$$

When considering optical fields it is generally simplest to think about the intensity of the light, which is related to the square of the electric field. The intensity \mathcal{I} is given by

$$\mathcal{I} = \frac{c\epsilon_0}{2} |\mathbf{E}_{\text{ac}}|^2. \quad (12)$$

The size of the light shift depends on the polarisation of the light and the frequency-dependent polarisability of the molecule α , which consists of a scalar, vector and tensor part α_k , $k = 0, 1, 2$. The scalar polarisability leads to an equal shift of all levels, which can be expressed as

$$U_0 = -\frac{\alpha_0}{2\epsilon_0 c} \mathcal{I} = -\alpha'_0 \mathcal{I}. \quad (13)$$

For simplicity we have introduced the reduced polarisability $\alpha'_k = \alpha_k / (2c\epsilon_0)$.

2. Package

The package contains two main notebooks. The first `Hamiltonian`, is used to build the Hamiltonians and the second `Calculate` uses eigenstates and eigenenergies found from diagonalising the Hamiltonian to run various calculations. We also include a file `Constants` which includes all of the required constants for CaF [53, 54, 55], as well as the constants required to calculate the field-free, Zeeman and dc electric field effects for BaF [56] and SrF [54, 57, 58].

2.1. Hamiltonian

We construct the Hamiltonian as a 2d array of size d ,

$$d = (2I + 1) \times (2S + 1) \times \sum_{N=0}^{N_{\max}} (2N + 1), \quad (14)$$

where N_{\max} is defined by the user as the maximum rotational level to be included in the calculation. A Hamiltonian is constructed using the `build` function, which takes N_{\max} (integer), `Constants` (dictionary) and `Zeeman`, `dc`, `ac` (Booleans) as parameters. The `Constants` term requires the importing of the chosen molecular species dictionary, e.g., ‘CaF’ from the constants file. The `Zeeman`, `dc`, `ac` must be set to either ‘True’ or ‘False’ depending on which external fields are needed for the calculation. If an external field value is zero, the time required for a calculation can be reduced by setting the associated Boolean to ‘False’. The full Hamiltonian can then be constructed by simply adding together $H_0 = H_{\text{rot}} + H_{\text{hf}}$ with the external Hamiltonians multiplied by their respective fields, i.e., magnetic field with H_{B} , electric field with H_{dc} and light intensity with H_{ac} . An excerpt of code to calculate the Zeeman energies for SrF is given in the Examples section.

2.2. Calculate

The calculate file contains a selection of functions which can be used to identify quantum numbers of eigenstates and calculate transition dipole moments and polarisabilities.

2.2.1. State identification

The function `np.linalg.eigh` calculates the eigenstates and eigenenergies of the Hamiltonian and outputs these in order according to eigenenergy

from lowest to highest. If two levels cross in energy, then this can lead to a misidentification of eigenstates. To overcome this we include the function `sort_smooth` [46], which takes the arrays of eigenenergies and eigenstates calculated over a range of external field values as an input. Eigenstates are tracked by ensuring maximal overlap as the external field is changed, and the eigenenergies are reordered as appropriate to match.

To assign the sorted eigenstates with appropriate F and m_F labels, the function `label_FmF_states` is provided within `calculate`. It takes the sorted set of eigenstates as an input, along with `N_max` (integer), `Constants` (dictionary) and the magnetic field at which the eigenstates and eigenenergies are calculated, `B` (integer/float/list/array)³, and returns the relevant (N, F, m_F) or (N, F) labels.

We first generate a list of possible $|N, J, F, m_F\rangle$ basis states, following the order these quantum numbers are cycled through when constructing the matrix representation of the Hamiltonian in the `hamiltonian` function. The i^{th} entry in a given eigenstate can therefore be assigned as the coefficient of the i^{th} basis state in this list. For each eigenstate, all basis states with negligible coefficients are removed. In the case when multiple basis states remain, these are checked to ensure consistency in F and m_F quantum numbers. If this condition is met, these values are returned as the F, m_F label for that eigenstate. In the case that m_F is not a good quantum number, only F labels will be output.

For simplicity, the function `solve` is also provided, combining the functionality of `np.linalg.eigh`, `sort_smooth` and optionally, `label_FmF_states`. As inputs, this function requires `H` (`np.array`), the matrix representation of the Hamiltonian to solve, alongside `N_max` (integer) and `Constants` (dictionary). (N, F, m_F) labels can also be generated by setting the argument `label` (Boolean) to `True` and providing an additional input, `B` (integer/float/list/array), the magnetic field value(s) at which the eigenstates and eigenenergies are to be calculated.

2.2.2. Transition dipole moments

A second function within `calculate` is `transition_dipole_moment` which calculates the transition dipole moment between two states. The function takes `N_max`, `Constants`, `M`, `states` and `gs` as inputs. Here, `gs` is the cho-

³A non-zero B field must be applied to lift the Zeeman sublevel degeneracies

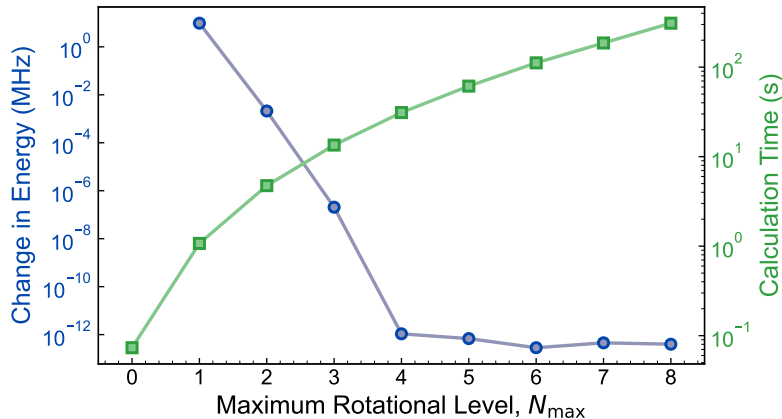


Figure 2: Plot showing the effect on the accuracy of energy calculation for $|N = 0, F = 0, m_F = 0\rangle$ (blue circles) and the time to run calculation (green squares) as the maximum rotational level N_{\max} considered is increased, up to 8 for CaF. The calculation is done with $\mathcal{I} = 2.5 \times 10^9 \text{ W m}^{-2}$, $E = 50 \text{ kV m}^{-1}$ and $B = 200 \text{ G}$.

sen ground state, **states** are the other states being considered, and **M** is the helicity of the transition such that $\mathbf{M} = +1, 0, -1$ for σ^+, π, σ^- transitions respectively. The function outputs the transition dipole moment in units of the molecule frame dipole moment d_0 . The first step is to calculate the induced dipole moment operator $\boldsymbol{\mu}$, using function **dipole**, the matrix representation of which is the same as for the dc electric field effect. We then calculate the expectation value between a chosen ground state **gs** and every other state via matrix multiplication using **np.einsum**.

2.2.3. Polarizability

We include a function **alpha_012** which calculates the scalar (α'_0), vector (α'_1) and tensor (α'_2) components of the reduced molecular polarizability at a given wavelength.

We make the assumption that only the lowest two electronic states i.e., $A^2\Pi$ and $B^2\Sigma^+$ contribute to the polarizability and don't include higher lying states in the calculation [59]. The function takes the wavelength of the light and **Constants** as inputs and generates a list of α'_k for $k = 0, 1, 2$ following the equations given in the Appendix.

2.3. Number of rotational states considered

In order to accurately determine eigenenergies, it is important to include an appropriate number of rotational levels, especially when considering large

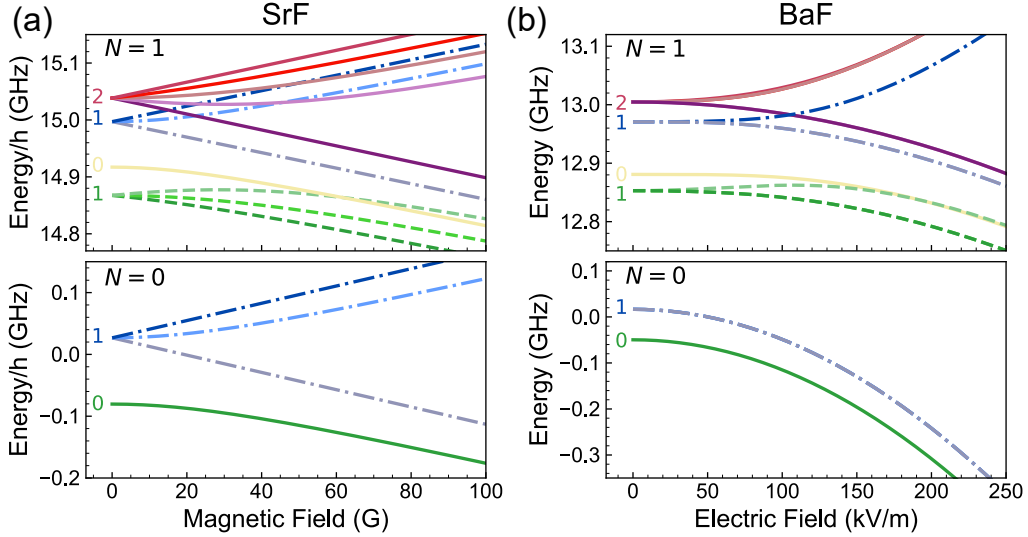


Figure 3: Plots showing (a) Zeeman effect for SrF molecules and (b) dc electric field shift for BaF molecules. The $N = 0$ states are shown in the lower panels and $N = 1$ states are shown in the upper panels. In each case only the plotted field is applied. The calculations include states up to $N = 4$. The line styles are set according to their F quantum number (labelled by the coloured number) and m_F levels are identified by the colour scale.

electric fields which cause rotational mixing. However, increasing the number of levels, N_{\max} , included in the calculation also increases the size of the associated Hilbert space and hence the length of time required for a calculation. The dependence of the calculated eigenenergies on N_{\max} is shown in figure 2. The blue circles show the change in the energy of the lowest energy state $|N = 0, F = 0, m_F = 0\rangle$ as N_{\max} is increased $\Delta E = (E(N_{\max}) - E(N_{\max} - 1))/h$. This is calculated for $\mathcal{I} = 2.5 \times 10^9 \text{ W m}^{-2}$, $E = 50 \text{ kV m}^{-1}$ and $B = 200 \text{ G}$. Once $N_{\max} \geq 4$ the change in energy is less than 10^{-12} MHz with the inclusion of an additional rotational level. Also shown in figure 2, as green squares, is the time taken to run these calculations on a laptop with 11th Gen Intel(R) Core(TM) i5-1135G7 @ 2.40 GHz with 32 GB of RAM. To achieve the required accuracy with $N_{\max} = 4$, the calculation time is still reasonable at around 30 seconds.

3. Examples

This section includes an excerpt of the code used to build and diagonalise a Hamiltonian and example energy calculations.

3.1. Zeeman effect and dc electric field shift

The first example considers the Zeeman effect for SrF. The Hamiltonian is constructed to use only the Zeeman contribution, the magnetic field values are defined and then applied to the Hamiltonian. The eigenstates, eigenenergies and state labels are then calculated using the `calc.solve` function. The code is as follows:

```
import numpy as np
import hamiltonian as hamiltonian
import calculate as calc
from constants import SrF

Nmax=4 #Identify the maximum N
H0,H_B,H_dc,H_ac
    = hamiltonian.build
      (Nmax,SrF,zeeman=True,Edc=False
       ,Eac=False)

B = np.linspace(0,100,5000)*1e-4 #Tesla

H = H_0[... , None] + H_B[... , None]*B
H = H.transpose(2,0,1)

energies, states, label_list =
    calc.solve(H, Nmax, SrF,label=True, B)
```

This code produces the data shown in figure 3(a). The magnetic field is varied from 0 to 100 G in steps of 2 mG, with no electric or light fields present. The $N = 0$ and $N = 1$ rotational levels are shown in separate panels as the rotational splitting is ≈ 15 GHz. In both panels, the splitting of the different m_F states can be clearly seen.

Similarly, the dc electric field shifts can be calculated by slightly adjusting the above code. Namely, changing the arguments passed to `build` such that `zeeman=False`, `Edc=True`, as well as replacing `H_B` with `H_dc` in the definition of the variable `H`. The results of this calculation for BaF are shown in figure 3(b). Here, the electric field is varied from 0 to 250 kV m⁻¹ in steps of

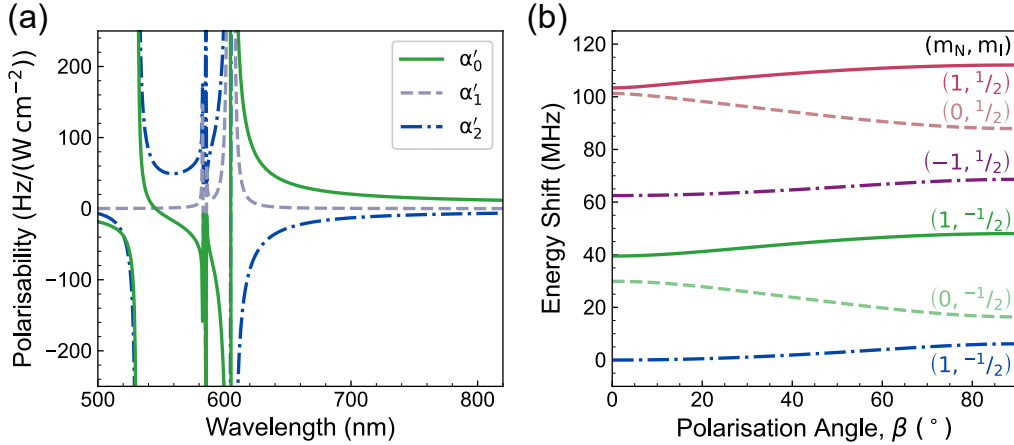


Figure 4: (a) Calculated polarisabilities for CaF in the ground electronic and vibrational state, $X(v = 0)$. The scalar component (α'_0) is shown in the solid green line, the vector component (α'_1) in the dashed grey line and the tensor component (α'_2) in the dash-dotted blue line. (b) ac light shift for CaF in the $N = 1, m_s = -1/2$ levels. Calculations are performed with a magnetic field of $B = 300$ G, and for linearly polarised 780 nm light at an angle β to the B field and an intensity of $\mathcal{I} = 30$ GW m $^{-2}$. The states are labeled by the m_N and m_I quantum numbers. Zero energy is defined to be the energy of the lowest energy state at $\beta = 0^\circ$

150 V m $^{-1}$, with no magnetic or light field present. Again, the results are separated into two panels according to rotational number. Comparing these panels to those in figure 3(a), it can be seen that the dc electric field does not lift the degeneracy between all m_F states.

3.2. Polarisability and light shift

The effect of off-resonant light is becoming increasingly important to understand as molecules are regularly being loaded into conservative optical traps, such as optical dipole traps and tweezers [60, 8]. To compute the light shift, we need the values of the polarisability components α'_k , which can either be set in the `constants` file or calculated using the `polarisability` function for a given wavelength. Figure 4(a) shows the three polarisability components calculated for CaF, using the `polarisability` function over a wavelength range of $\lambda = 500$ nm to $\lambda = 820$ nm.

Additionally, the light shift can be calculated similarly to the Zeeman and dc electric field shifts by modifying the `build` function. Figure 4(b) shows an example for CaF molecules. The calculations were done using linearly

	(1,1,-1)	(1,0,0)	(1,1,1)	(1,2,-2)	(1,2,2)
(0,0,0)	0.561	0.0	0.135	0.0	0.0
(0,1,-1)	0.096	0.333	0.0	0.577	0.0
(0,1,0)	0.096	0.333	0.397	0.0	0.0
(0,1,1)	0.0	0.333	0.397	0.0	0.577
(2,2,2)	0.0	0.0	0.05	0.0	0.092
(2,2,1)	0.0	0.0	0.036	0.0	0.065
(2,2,0)	0.253	0.0	0.021	0.0	0.0
(2,2,-1)	0.439	0.0	0.0	0.065	0.0
(2,2,-2)	0.62	0.0	0.0	0.092	0.0
(2,1,1)	0.0	0.471	0.281	0.0	0.082
(2,1,0)	0.068	0.471	0.281	0.0	0.0
(2,1,-1)	0.068	0.471	0.0	0.082	0.0
(2,2,-2)	0.098	0.0	0.0	0.241	0.0
(2,2,-1)	0.069	0.0	0.0	0.171	0.0
(2,2,0)	0.04	0.0	0.225	0.0	0.0
(2,2,1)	0.0	0.0	0.389	0.0	0.171
(2,2,2)	0.0	0.0	0.55	0.0	0.241
(2,3,-3)	0.0	0.0	0.0	0.632	0.0
(2,3,-2)	0.0	0.0	0.0	0.365	0.0
(2,3,-1)	0.0	0.0	0.0	0.163	0.0
(2,3,0)	0.0	0.0	0.0	0.0	0.0
(2,3,1)	0.0	0.0	0.0	0.0	0.163
(2,3,2)	0.0	0.0	0.0	0.0	0.365
(2,3,3)	0.0	0.0	0.0	0.0	0.632

Figure 5: Table showing the transition dipole moments in units of molecular dipole between some $N = 1$ states, shown in columns and all $N = 0, 2$ states, shown in rows for CaF. Labels are in the form (N, F, m_F) . The relative intensity of each transition is given by the cell value, and highlighted by the colour, with darker colours indicating stronger transitions. Red, green and blue are chosen to represent coupling fields with polarisations that drive σ^+ , π and σ^- transitions respectively.

polarised light field of wavelength 780 nm, intensity 30 GW m⁻² with a magnetic field of 300 G and no electric field. We plot the energy shift against the angle (β) between the polarisation of the light and the applied magnetic field from 0 to 90° relative to the lowest energy state at $\beta = 0$. Here we identify the levels by m_N and m_I .

3.3. Transition Dipole Moments

Rotational transitions in molecules can readily be driven by microwave fields. To understand the strength of these transitions one needs to calculate the transition dipole moment (TDM), which can be done using the function `transition_dipole_moment`. Figure 5 shows the TDM from a selection of $N = 1$ states ($|1, 1, -1\rangle, |1, 0, 0\rangle, |1, 1, 1\rangle, |1, 2, -2\rangle$ and $|1, 2, 2\rangle$) to all states in rotational levels $N = 0, 2$ of CaF. Transitions from $N = 1$ are considered as this is the state occupied following laser slowing. The strength of each transition is given in the cell, and highlighted by the colour. The red, green and blue sequential colour maps indicate the relative strengths for σ^+ , π and σ^- transitions respectively. The calculations were done in the presence of an magnetic field of 60 mG.

4. Conclusion

We have written a Python package to construct the Hamiltonian and calculate eigenenergies and eigenstates of $^2\Sigma$ state of molecules in the presence of external fields. The package is of particular relevance to molecules which can be laser cooled and we have provided constants for CaF, SrF and BaF molecules. As more molecular species are investigated, further constants can be added. Future iterations of the package could also be made to include an angle variable for magnetic and electric fields.

5. Code Availability and Installation

The DiPolMol-Py files are available to download from the github repository [61].

6. Acknowledgements

We thank Phil Gregory, Mike Tarbutt, Luke Caldwell, Jeremy Hutson and Simon Cornish for helpful discussions. Thank you also to Archie Baldock for testing of the package.

This work was supported by UKRI and EPSRC Grants: MR/X033430/1 and EP/X013758/1.

Appendix A.

Here we give the matrix elements for the various Hamiltonians included in the package. For brevity we use $|i\rangle$ as shorthand for the basis state $|N, J, F, m_F\rangle$.

Appendix A.1. Field-free Hamiltonian

The rotational Hamiltonian is diagonal in our basis so can easily be written as

$$\begin{aligned} \langle i' | H_{\text{rot}} | i \rangle = & B_v N(N+1) \delta_{N,N'} \delta_{J,J'} \delta_{F,F'} \delta_{m_F,m'_F} \\ & + D_v (N(N+1))^2 \delta_{N,N'} \delta_{J,J'} \delta_{F,F'} \delta_{m_F,m'_F}. \end{aligned} \tag{A.1}$$

The hyperfine Hamiltonian can be divided into four terms which are expressed as:

$$\langle i' | \gamma \mathbf{S} \cdot \mathbf{N} | i \rangle = \frac{\gamma}{2} (J(J+1) - N(N+1) - \frac{3}{4}) \delta_{N,N'} \delta_{J,J'} \delta_{F,F'} \delta_{m_F,m'_F}, \quad (\text{A.2})$$

$$\begin{aligned} \langle i' | (b+c/3) \mathbf{I} \cdot \mathbf{S} | i \rangle &= (-1)^{J+J'+F+N} \delta_{N,N'} \delta_{F,F'} \delta_{m_F,m'_F} \\ &\times \frac{3}{2} ((2J+1)(2J'+1))^{\frac{1}{2}} \begin{Bmatrix} J' & \frac{1}{2} & F \\ \frac{1}{2} & J & 1 \end{Bmatrix}, \end{aligned} \quad (\text{A.3})$$

$$\begin{aligned} \langle i' | \frac{\sqrt{6}c}{3} T^2(C) \cdot T^2(\mathbf{I}, \mathbf{S}) | i \rangle &= \sqrt{10}c (-1)^{J+F+N'+\frac{1}{2}} \delta_{F,F'} \delta_{m_F,m'_F} ((2N+1)(2N'+1)) \\ &\times (2J+1)(2J'+1)^{\frac{1}{2}} \begin{Bmatrix} J' & \frac{1}{2} & F \\ \frac{1}{2} & J & 1 \end{Bmatrix} \begin{Bmatrix} J' & J & 1 \\ \frac{1}{2} & \frac{3}{2} & N \end{Bmatrix} \\ &\times \begin{Bmatrix} N & N' & 2 \\ \frac{1}{2} & \frac{3}{2} & J' \end{Bmatrix} \begin{pmatrix} N' & 2 & N \\ 0 & 0 & 0 \end{pmatrix}, \end{aligned} \quad (\text{A.4})$$

$$\begin{aligned} \langle i' | c_F \mathbf{I} \cdot \mathbf{N} | i \rangle &= (-1)^{2J'+F+N} \delta_{N,N'} \delta_{F,F'} \delta_{m_F,m'_F} \\ &\times \left(\frac{3}{2} (2J+1)(2J'+1)N(N+1)(2N+1) \right)^{\frac{1}{2}} \\ &\times \begin{Bmatrix} J' & \frac{1}{2} & F \\ \frac{1}{2} & J & 1 \end{Bmatrix} \begin{Bmatrix} N' & J' & \frac{1}{2} \\ J & N & 1 \end{Bmatrix}. \end{aligned} \quad (\text{A.5})$$

Appendix B. External field Hamiltonian

Next we consider the Zeeman Hamiltonian which can be decomposed into four terms in the following way for a magnetic field aligned along z . The second term is most naturally evaluated in Hund's case (a) basis, with the projections of L and S along the internuclear axis being given by Λ and Σ and we can define $\Omega = \Lambda + \Sigma$. As $L = 0$ we also have $\Lambda = 0$, this means that $\Omega = \Sigma = \pm \frac{1}{2}$. We then transform the basis back into Hund's case (b). The

four terms are

$$\begin{aligned}
\langle i' | (g_s \mu_B + g_l \mu_B) \mathbf{S} \cdot \mathbf{B} | i \rangle &= B_z \sqrt{\frac{3}{2}} (g_s \mu_B + g_l \mu_B) \times (-1)^{(J'+J+F'+F-m_F+3+N')} \\
&\times \delta_{N,N'} ((2F+1)(2F'+1)(2J+1)(2J'+1))^{\frac{1}{2}} \\
&\times \begin{pmatrix} F' & 1 & F \\ -m'_F & 0 & m_F \end{pmatrix} \begin{Bmatrix} J' & F' & \frac{1}{2} \\ F & J & 1 \end{Bmatrix} \begin{Bmatrix} \frac{1}{2} & J' & N \\ J & \frac{1}{2} & 1 \end{Bmatrix},
\end{aligned} \tag{B.1}$$

$$\begin{aligned}
\langle i' | g_l \mu_B (\mathbf{S} \cdot \lambda) (\mathbf{B} \cdot \lambda) | i \rangle &= B_z g_l \mu_B (-1)^{(F+F'-m'_F+2J'+N+N'+\frac{1}{2})} \\
&\times ((2F+1)(2F'+1)(2J+1)(2J'+1))^{\frac{1}{2}} \\
&\times ((2N+1)(2N'+1))^{\frac{1}{2}} \begin{Bmatrix} J & F & \frac{1}{2} \\ F' & J' & 1 \end{Bmatrix} \begin{pmatrix} F' & 1 & F \\ -m'_F & 0 & m_F \end{pmatrix} \\
&\times \sum_{\Omega=-\frac{1}{2}}^{\frac{1}{2}} (-1)^\Omega \begin{pmatrix} J' & 1 & J \\ -\Omega & 0 & \Omega \end{pmatrix} \begin{pmatrix} J & S & N \\ \Omega & -\Omega & 0 \end{pmatrix} \begin{pmatrix} J' & S' & N' \\ \Omega & -\Omega & 0 \end{pmatrix} \Omega,
\end{aligned} \tag{B.2}$$

$$\begin{aligned}
\langle i' | (g_r \mu_B) \mathbf{N} \cdot \mathbf{B} | i \rangle &= B_z g_r \mu_B \times (-1)^{(J+J'+F+F'-m'_F+3+N')} \delta_{N,N'} \\
&\times ((2F+1)(2F'+1)(2J+1)(2J'+1))^{\frac{1}{2}} \\
&\times \begin{pmatrix} F' & 1 & F \\ -m'_F & 0 & m_F \end{pmatrix} \begin{Bmatrix} J' & F' & \frac{1}{2} \\ F & J & 1 \end{Bmatrix} \begin{Bmatrix} N & J & \frac{1}{2} \\ J' & N' & 1 \end{Bmatrix},
\end{aligned} \tag{B.3}$$

$$\begin{aligned}
\langle i' | (g_N \mu_N) \mathbf{I} \cdot \mathbf{B} | i \rangle &= B_z g_N \mu_N \times (-1)^{(J'+2F'-m'_F+3/2)} \delta_{J,J'} \\
&\times \left(\frac{3}{2} (2F+1)(2F'+1) \right)^{\frac{1}{2}} \\
&\times \begin{pmatrix} F' & 1 & F \\ -m'_F & 0 & m_F \end{pmatrix} \begin{Bmatrix} \frac{1}{2} & F & J \\ F' & \frac{1}{2} & 1 \end{Bmatrix}.
\end{aligned} \tag{B.4}$$

Under application of an external electric field of amplitude E the dc

electric field Hamiltonian is represented as

$$\begin{aligned}
\langle i' | \mu_e \mathbf{E} \cdot \mathbf{z} | i \rangle &= \mu_e E (-1)^{(F' - m'_F + F + J' + J + 2N' + 1)} ((2F + 1)(2F' + 1)) \\
&\quad \times (2J + 1)(2J' + 1)(2N + 1)(2N' + 1)^{\frac{1}{2}} \\
&\quad \times \begin{Bmatrix} J & F & \frac{1}{2} \\ F' & J' & 1 \end{Bmatrix} \begin{Bmatrix} N & J & \frac{1}{2} \\ J' & N' & 1 \end{Bmatrix} \begin{pmatrix} F' & 1 & F \\ -m'_F & 0 & m_F \end{pmatrix} \\
&\quad \times \begin{pmatrix} N' & 1 & N \\ 0 & 0 & 0 \end{pmatrix}.
\end{aligned} \tag{B.5}$$

The matrix elements for the ac electric field effect under an applied off-resonant light field with frequency ω_L are derived in [62] and given here. $D_{M,0}^2$ is the Wigner D-matrix allowing rotation of the polarisation of the light which is important for the anisotropic light shift only. The total light shift experienced by the molecule is a sum over $k = 0, 1, 2$, given by

$$\begin{aligned}
\langle i' | H_{ac}^k | i \rangle &= D_{M,0}^2(0, \beta, 0) \times (-1)^{(F' - m'_F + F - J' + J + 1)} ((2F + 1)(2F' + 1)) \\
&\quad \times (2J + 1)(2J' + 1)(2N + 1)(2N' + 1)^{\frac{1}{2}} \begin{Bmatrix} J' & F' & \frac{1}{2} \\ F & J & K \end{Bmatrix} \\
&\quad \times \begin{pmatrix} F' & K & F \\ -m'_F & P & m_F \end{pmatrix} \begin{pmatrix} J & \frac{1}{2} & N \\ -\frac{1}{2} & \frac{1}{2} & 0 \end{pmatrix} \begin{pmatrix} J' & \frac{1}{2} & N' \\ -\frac{1}{2} & \frac{1}{2} & 0 \end{pmatrix} \\
&\quad \times \begin{pmatrix} J' & K & J \\ -\frac{1}{2} & 0 & \frac{1}{2} \end{pmatrix} \alpha'_k.
\end{aligned} \tag{B.6}$$

To calculate the components of the molecular polarisability we first calculate the molecule-frame parallel α_{\parallel} and perpendicular polarisability α_{\perp} components. In this package we consider only contributions from the X, A and B states. This gives us two expressions for α_{\perp} for $\Omega = \frac{1}{2}, \frac{3}{2}$, which are

$$\alpha_{\parallel} = \sum_j \left(\frac{1}{\hbar(\omega_j + \omega_L)} + \frac{1}{\hbar(\omega_j - \omega_L)} \right) d_{X,j}, \tag{B.7}$$

$$\alpha_{\perp,\Omega} = \sum_j \left(\frac{1}{\hbar(\omega_{k,\Omega} + \omega_L)} + \frac{1}{\hbar(\omega_j - \omega_{k,\Omega})} \right) d_{X,k}, \tag{B.8}$$

$$\alpha_{\perp} = \frac{1}{2} \left(\alpha_{\perp,\frac{1}{2}} + \alpha_{\perp,\frac{3}{2}} \right), \tag{B.9}$$

where $d_{X,j}$ and $d_{X,k}$ are the transition dipole moments between the $X(v = 0)$ state and included excited states. These are summed over $j = X(v = 1), B(v = 0)$ and $k = A(v = 0), A(v = 1)$, respectively. The scalar, vector and tensor components of the polarisability can then be calculated. The equations describing these are

$$\alpha_0 = \frac{1}{3} (\alpha_{\parallel} + 2\alpha_{\perp}), \quad (\text{B.10})$$

$$\alpha_1 = \frac{1}{2} \left(\frac{\omega_L}{\omega_{\frac{1}{2}}} \alpha_{\perp, \frac{1}{2}} + \frac{\omega_L}{\omega_{\frac{3}{2}}} \alpha_{\perp, \frac{3}{2}} \right), \quad (\text{B.11})$$

$$\alpha_2 = \frac{2}{3} (\alpha_{\parallel} - \alpha_{\perp}). \quad (\text{B.12})$$

References

- [1] J. Lim, J. R. Almond, M. A. Trigatzis, J. A. Devlin, N. J. Fitch, B. E. Sauer, M. R. Tarbutt, E. A. Hinds, Laser cooled YbF molecules for measuring the electron’s electric dipole moment, *Phys. Rev. Lett.* 120 (2018) 123201. doi:10.1103/PhysRevLett.120.123201.
- [2] P. Aggarwal, H. L. Bethlem, A. Borschevsky, M. Denis, K. Esajas, P. A. Haase, Y. Hao, S. Hoekstra, K. Jungmann, T. B. Meijknecht, M. C. Mooij, R. G. Timmermans, W. Ubachs, L. Willmann, A. Zapara, Measuring the electric dipole moment of the electron in BaF, *Eur. Phys. J. D* 72 (2018) 197. doi:10.1140/epjd/e2018-90192-9.
- [3] L. Anderegg, N. B. Vilas, C. Hallas, P. Robichaud, A. Jadbabaie, J. M. Doyle, N. R. Hutzler, Quantum control of trapped polyatomic molecules for eEDM searches, *Science* 382 (6671) (2023) 665–668. doi:10.1126/science.adg8155.
- [4] T. S. Roussy, L. Caldwell, T. Wright, W. B. Cairncross, Y. Shagam, K. B. Ng, N. Schlossberger, S. Y. Park, A. Wang, J. Ye, E. A. Cornell, An improved bound on the electron’s electric dipole moment, *Science* 381 (6653) (2023) 46–50. doi:10.1126/science.adg4084.
- [5] O. Grasdijk, O. Timgren, J. Kastelic, T. Wright, S. Lamoreaux, D. Demille, K. Wenz, M. Aitken, T. Zelevinsky, T. Winick, D. Kawall, CeN-TREX: A new search for time-reversal symmetry violation in the ^{205}Tl

- nucleus, *Quantum Sci. and Tech.* 6 (2021) 044007. doi:10.1088/2058-9565/abdca3.
- [6] G. Barontini, L. Blackburn, V. Boyer, F. Butuc-Mayer, X. Calmet, J. R. Crespo López-Urrutia, E. A. Curtis, B. Darquié, J. Dunningham, N. J. Fitch, E. M. Forgan, K. Georgiou, P. Gill, R. M. Godun, J. Goldwin, V. Guarrera, A. C. Harwood, I. R. Hill, R. J. Hendricks, M. Jeong, M. Y. H. Johnson, M. Keller, L. P. Kozhiparambil Sajith, F. Kuipers, H. S. Margolis, C. Mayo, P. Newman, A. O. Parsons, L. Prokhorov, B. I. Robertson, J. Rodewald, M. S. Safronova, B. E. Sauer, M. Schioppo, N. Sherrill, Y. V. Stadnik, K. Szymaniec, M. R. Tarbutt, R. C. Thompson, A. Tofful, J. Tunesi, A. Vecchio, Y. Wang, S. Worm, Measuring the stability of fundamental constants with a network of clocks, *EPJ Quantum Tech.* 9 (2022) 12. doi:10.1140/epjqt/s40507-022-00130-5.
- [7] B. Yan, S. A. Moses, B. Gadway, J. P. Covey, K. R. Hazzard, A. M. Rey, D. S. Jin, J. Ye, Observation of dipolar spin-exchange interactions with lattice-confined polar molecules, *Nature* 501 (2013) 521–525. doi:10.1038/nature12483.
- [8] C. M. Holland, Y. Lu, L. W. Cheuk, On-demand entanglement of molecules in a reconfigurable optical tweezer array, *Science* 382 (6675) (2023) 1143–1147. doi:10.1126/science.adf4272.
- [9] Y. Bao, S. S. Yu, L. Anderegg, E. Chae, W. Ketterle, K.-K. Ni, J. M. Doyle, Dipolar spin-exchange and entanglement between molecules in an optical tweezer array, *Science* 382 (6675) (2023) 1138–1143. doi:10.1126/science.adf8999.
- [10] D. K. Ruttley, T. R. Hepworth, A. Guttridge, S. L. Cornish, Long-lived entanglement of molecules in magic-wavelength optical tweezers, *Nature* 637 (2024) 827–832. doi:10.1038/s41586-024-08365-1.
- [11] L. R. B. Picard, A. J. Park, G. E. Patenotte, S. Gebretsadkan, D. Wellnitz, A. M. Rey, K.-K. Ni, Sub-millisecond entanglement and iSWAP gate between molecular qubits, *Nature* 637 (2024) 821–826. doi:10.1038/s41586-024-08177-3.
- [12] H. J. Williams, L. Caldwell, N. J. Fitch, S. Truppe, J. Rodewald, E. A. Hinds, B. E. Sauer, M. R. Tarbutt, Magnetic trapping and coherent

- control of laser-cooled molecules, *Phys. Rev. Lett.* 120 (2018) 163201. doi:10.1103/PhysRevLett.120.163201.
- [13] S. Burchesky, L. Anderegg, Y. Bao, S. S. Yu, E. Chae, W. Ketterle, K.-K. Ni, J. M. Doyle, Rotational coherence times of polar molecules in optical tweezers, *Phys. Rev. Lett.* 127 (2021) 123202. doi:10.1103/PhysRevLett.127.123202.
- [14] A. J. Park, L. R. Picard, G. E. Patenotte, J. T. Zhang, T. Rosenband, K.-K. Ni, Extended rotational coherence of polar molecules in an elliptically polarized trap, *Phys. Rev. Lett.* 131 (2023) 183401. doi:10.1103/PhysRevLett.131.183401.
- [15] P. D. Gregory, L. M. Fernley, A. L. Tao, S. L. Bromley, J. Stepp, Z. Zhang, S. Kotochigova, K. R. A. Hazzard, S. L. Cornish, Second-scale rotational coherence and dipolar interactions in a gas of ultracold polar molecules, *Nat. Phys.* 20 (2024) 415–421. doi:10.1038/s41567-023-02328-5.
- [16] D. DeMille, Quantum computation with trapped polar molecules, *Phys. Rev. Lett.* 88 (2002) 067901. doi:10.1103/PhysRevLett.88.067901.
- [17] L. D. Carr, D. DeMille, R. V. Krems, J. Ye, Cold and ultracold molecules: science, technology and applications, *New J. Phys.* 11 (2009) 055049. doi:10.1088/1367-2630/11/5/055049.
- [18] K. R. Hazzard, S. R. Manmana, M. Foss-Feig, A. M. Rey, Far-from-equilibrium quantum magnetism with ultracold polar molecules, *Phys. Rev. Lett.* 110 (2013) 075301. doi:10.1103/PhysRevLett.110.075301.
- [19] K. R. Hazzard, B. Gadway, M. Foss-Feig, B. Yan, S. A. Moses, J. P. Covey, N. Y. Yao, M. D. Lukin, J. Ye, D. S. Jin, A. M. Rey, Many-body dynamics of dipolar molecules in an optical lattice, *Phys. Rev. Lett.* 113 (2014) 195302. doi:10.1103/PhysRevLett.113.195302.
- [20] S. L. Cornish, M. R. Tarbutt, K. R. A. Hazzard, Quantum computation and quantum simulation with ultracold molecules, *Nat. Phys.* 20 (2024) 730–740. doi:10.1038/s41567-024-02453-9.

- [21] B. Sundar, B. Gadway, K. R. A. Hazzard, Synthetic dimensions in ultracold polar molecules, *Sci. Rep.* 8 (2018) 3422. doi:10.1038/s41598-018-21699-x.
- [22] C. Feng, H. Manetsch, V. G. Rousseau, K. R. A. Hazzard, R. Scalettar, Quantum membrane phases in synthetic lattices of cold molecules or Rydberg atoms, *Phys. Rev. A* 105 (2022) 063320. doi:10.1103/PhysRevA.105.063320.
- [23] R. Sawant, J. A. Blackmore, P. D. Gregory, J. Mur-Petit, D. Jaksch, J. Aldegunde, J. M. Hutson, M. R. Tarbutt, S. L. Cornish, Ultracold polar molecules as qudits, *New J. Phys.* 22 (2020) 013027. doi:10.1088/1367-2630/ab60f4.
- [24] J. Toscano, H. J. Lewandowski, B. R. Heazlewood, Cold and controlled chemical reaction dynamics, *Phys. Chem. Chem. Phys.* 22 (2020) 9180–9194. doi:10.1039/d0cp00931h.
- [25] B. R. Heazlewood, T. P. Softley, Towards chemistry at absolute zero, *Nat. Rev. Chem.* 5 (2021) 125–140. doi:10.1038/s41570-020-00239-0.
- [26] Y. Liu, K.-K. Ni, Bimolecular chemistry in the ultracold regime, *Ann. Rev. Phys. Chem.* 73 (2022) 73–96. doi:10.1146/annurev-physchem-090419-043244.
- [27] L. W. Cheuk, L. Anderegg, Y. Bao, S. Burchesky, S. S. Yu, W. Ketterle, K. K. Ni, J. M. Doyle, Observation of collisions between two ultracold ground-state CaF molecules, *Phys. Rev. Lett.* 125 (2020) 043401. doi:10.1103/PhysRevLett.125.043401.
- [28] S. Jurgilas, A. Chakraborty, C. J. H. Rich, L. Caldwell, H. J. Williams, N. J. Fitch, B. E. Sauer, M. D. Frye, J. M. Hutson, M. R. Tarbutt, Collisions between ultracold molecules and atoms in a magnetic trap, *Phys. Rev. Lett.* 126 (2021) 153401. doi:10.1103/PhysRevLett.126.153401.
- [29] M. Koller, F. Jung, J. Phrompao, M. Zeppenfeld, I. M. Rabey, G. Rempe, Electric-field-controlled cold dipolar collisions between trapped CH₃F molecules, *Phys. Rev. Lett.* 128 (2022) 203401. doi:10.1103/PhysRevLett.128.203401.

- [30] M. D. D. Rosa, Laser-cooling molecules: Concept, candidates, and supporting hyperfine-resolved measurements of rotational lines in the A-X(0,0) band of CaH, *Eur. Phys. J. D* 31 (2004) 395–402. doi:10.1140/epjd/e2004-00167-2.
- [31] J. F. Barry, D. J. McCarron, E. B. Norrgard, M. H. Steinecker, D. Demille, Magneto-optical trapping of a diatomic molecule, *Nature* 512 (2014) 286–289. doi:10.1038/nature13634.
- [32] S. Truppe, H. J. Williams, M. Hambach, L. Caldwell, N. J. Fitch, E. A. Hinds, B. E. Sauer, M. R. Tarbutt, Molecules cooled below the Doppler limit, *Nature Physics* 13 (2017) 1173–1176. doi:10.1038/nphys4241.
- [33] L. Anderegg, B. L. Augenbraun, E. Chae, B. Hemmerling, N. R. Hutzler, A. Ravi, A. Collopy, J. Ye, W. Ketterle, J. M. Doyle, Radio frequency magneto-optical trapping of CaF with high density, *Phys. Rev. Lett.* 119 (2017) 103201. doi:10.1103/PhysRevLett.119.103201.
- [34] A. L. Collopy, S. Ding, Y. Wu, I. A. Finneran, L. Anderegg, B. L. Augenbraun, J. M. Doyle, J. Ye, 3D magneto-optical trap of yttrium monoxide, *Phys. Rev. Lett.* 121 (2018) 213201. doi:10.1103/PhysRevLett.121.213201.
- [35] N. B. Vilas, C. Hallas, L. Anderegg, P. Robichaud, A. Winnicki, D. Mitra, J. M. Doyle, Magneto-optical trapping and sub-Doppler cooling of a polyatomic molecule, *Nature* 606 (2022) 70–74. doi:10.1038/s41586-022-04620-5.
- [36] Z. D. Lasner, A. Frenett, H. Sawaoka, L. Anderegg, B. Augenbraun, H. Lampson, M. Li, A. Lunstad, J. Mango, A. Nasir, T. Ono, T. Sakamoto, J. M. Doyle, Magneto-optical trapping of a heavy polyatomic molecule for precision measurement, *Phys. Rev. Lett.* 134 (2025) 083401. doi:10.1103/PhysRevLett.134.083401.
- [37] Z. Zeng, S. Deng, S. Yang, B. Yan, Three-dimensional magneto-optical trapping of barium monofluoride, *Phys. Rev. Lett.* 133 (2024) 143404. doi:10.1103/PhysRevLett.133.143404.
- [38] X. Alauze, J. Lim, M. A. Trigatzis, S. Swarbrick, F. J. Collings, N. J. Fitch, B. E. Sauer, M. R. Tarbutt, An ultracold molecular beam for

- testing fundamental physics, *Quantum Sci. Tech.* 6 (2021) 044005. doi:10.1088/2058-9565/ac107e.
- [39] F. Kogel, M. Rockenhäuser, R. Albrecht, T. Langen, A laser cooling scheme for precision measurements using fermionic barium monofluoride ($^{137}\text{Ba}^{19}\text{F}$) molecules, *New J. Phys.* 23 (2021) 095003. doi:10.1088/1367-2630/ac1df2.
- [40] S. F. Vázquez-Carson, Q. Sun, J. Dai, D. Mitra, T. Zelevinsky, Direct laser cooling of calcium monohydride molecules, *New J. Phys.* 24 (2022) 083006. doi:10.1088/1367-2630/ac806c.
- [41] J. Dai, Q. Sun, B. C. Riley, D. Mitra, T. Zelevinsky, Laser cooling of a fermionic molecule, *Phys. Rev. Res.* 6 (2024) 033135. doi:10.1103/PhysRevResearch.6.033135.
- [42] N. H. Pilgram, B. W. Baldwin, D. S. L. Mantia, S. P. Eckel, E. B. Norrgard, Spectroscopy of laser-cooling transitions in MgF, *Phys. Rev. A* 110 (2024) 023110. doi:10.1103/PhysRevA.110.023110.
- [43] S. Hofsäss, M. Doppelbauer, S. C. Wright, S. Kray, B. G. Sartakov, J. Pérez-Ríos, G. Meijer, S. Truppe, Optical cycling of AlF molecules, *New J. Phys.* 23 (2021) 075001. doi:10.1088/1367-2630/ac06e5.
- [44] E. B. Norrgard, E. R. Edwards, D. J. McCarron, M. H. Steinecker, D. DeMille, S. S. Alam, S. K. Peck, N. S. Wadia, L. R. Hunter, Hyperfine structure of the $B^3\Pi_1$ state and predictions of optical cycling behavior in the $X \rightarrow B$ transition of TlF, *Phys. Rev. A* 95 (2017) 062506. doi:10.1103/PhysRevA.95.062506.
- [45] J. C. Schnaubelt, J. C. Shaw, D. J. McCarron, Cold CH radicals for laser cooling and trapping (2021). arXiv:2109.03953.
- [46] J. A. Blackmore, P. D. Gregory, J. M. Hutson, S. L. Cornish, Diatomicpy: A Python module for calculating the rotational and hyperfine structure of $^1\Sigma$ molecules, *Computer Physics Communications* 282 (2023) 108512. doi:10.1016/j.cpc.2022.108512.
- [47] A. Ciamei, J. Szczepkowski, A. Bayerle, V. Barbé, L. Reichsöllner, S. M. Tzanova, C.-C. Chen, B. Pasquiou, A. Grochola, P. Kowalczyk, W. Jastrzebski, F. Schreck, The RbSr $^2\Sigma^+$ ground state investigated via spec-

- troscopy of hot and ultracold molecules, *Phys. Chem. Chem. Phys.* 20 (2018) 26221–26240. doi:10.1039/C8CP03919D.
- [48] T. Franzen, B. Pollklesener, C. Sillus, A. Görlitz, Intercombination-line photoassociation spectroscopy of $^{87}\text{Rb}^{170}\text{Yb}$, *Phys. Rev. A* 107 (2023) 023114. doi:10.1103/PhysRevA.107.023114.
- [49] A. Guttridge, S. A. Hopkins, M. D. Frye, J. J. McFerran, J. M. Hutson, S. L. Cornish, Production of ultracold Cs*Yb molecules by photoassociation, *Phys. Rev. A* 97 (2018) 063414. doi:10.1103/PhysRevA.97.063414.
- [50] A. Green, J. H. See Toh, R. Roy, M. Li, S. Kotochigova, S. Gupta, Two-photon photoassociation spectroscopy of the $^2\Sigma^+$ YbLi molecular ground state, *Phys. Rev. A* 99 (2019) 063416. doi:10.1103/PhysRevA.99.063416.
- [51] J. M. Brown, A. Carrington, *Rotational Spectroscopy of Diatomic Molecules*, Cambridge University Press, 2010.
- [52] R. A. Frosch, H. M. Foley, Magnetic hyperfine structure in diatomic molecules, *Phys. Rev.* 88 (1952) 1337–1349. doi:10.1103/PhysRev.88.1337.
- [53] L. A. Kaledin, J. C. Bloch, M. C. McCarthy, R. W. Field, Analysis and Deperturbation of the $A^2\Pi$ and $B^2\Sigma^+$ States of CaF, *J. Mol. Spectrosc.* 197 (2) (1999) 289–296. doi:10.1006/jmsp.1999.7909.
- [54] P. J. Dagdigian, H. W. Cruse, R. N. Zare, Radiative lifetimes of the alkaline earth monohalides, *J. Chem. Phys.* 60 (1974) 2330–2339. doi:10.1063/1.1681366.
- [55] T. E. Wall, J. F. Kanem, J. J. Hudson, B. E. Sauer, D. Cho, M. G. Boshier, E. A. Hinds, M. R. Tarbutt, Lifetime of the $A(v' = 0)$ state and Franck-Condon factor of the $A-X(0-0)$ transition of CaF measured by the saturation of laser-induced fluorescence, *Phys. Rev. A* 78 (2008) 062509. doi:10.1103/PhysRevA.78.062509.
- [56] T. Chen, W. Bu, B. Yan, Structure, branching ratios, and a laser-cooling scheme for the BaF 138 molecule, *Phys. Rev. A* 94 (2016) 063415. doi:10.1103/PhysRevA.94.063415.

- [57] L.-E. Berg, K. Ekvall, T. Hansson, A. Iwamae, V. Zengin, D. Husain, P. Royen, Time-resolved measurements of the $B^2\Sigma$ state of SrF by laser spectroscopy, *Chemical Physics Letters* 248 (3) (1996) 283–288. doi:10.1016/0009-2614(95)01330-X.
- [58] W. Childs, L. Goodman, I. Renhorn, Radio-frequency optical double-resonance spectrum of SrF: The $X^2\Sigma^+$ state, *Journal of Molecular Spectroscopy* 87 (2) (1981) 522–533. doi:10.1016/0022-2852(81)90422-7.
- [59] L. Caldwell, M. R. Tarbutt, A general approach to state-dependent optical tweezer traps for polar molecules, *Phys. Rev. Res.* 3 (2020) 013291. doi:10.1103/PhysRevResearch.3.013291.
- [60] L. Anderegg, L. W. Cheuk, Y. Bao, S. Burchesky, W. Ketterle, K.-K. Ni, J. M. Doyle, An optical tweezer array of ultracold molecules, *Science* 365 (2019) 1156–1158. doi:10.1126/science.aax1265.
- [61] H. J. Williams, durham-qlm/dipolmol (2025).
URL <https://github.com/durham-qlm/DiPolMol>
- [62] L. Caldwell, M. R. Tarbutt, Sideband cooling of molecules in optical traps, *Physical Review Research* 2 (2020). doi:10.1103/PhysRevResearch.2.013251.